

The effect of local reinforcing bar reductions and anchorage zone cracking on the load capacity of RC half-joints



Pieter Desnerck*, Janet M. Lees, Chris T. Morley

University of Cambridge, Department of Engineering, Concrete and Composites Structures Group, Trumpington Street, CB2 1PZ Cambridge, United Kingdom

ARTICLE INFO

Article history:

Received 11 October 2016

Revised 9 July 2017

Accepted 12 September 2017

Available online 7 October 2017

Keywords:

Assessment
Dapped-end beam
Half-joint
Strut-and-tie
Load-bearing capacity
Corrosion
Anchorage
Cracking
Re-entrant corner

ABSTRACT

Half-joint beams, also referred to as dapped-end beams, have been the subject of several studies, primarily focussing on the design optimisation of new reinforced concrete beams and bridge decks. Existing half-joint structures, however, often show signs of deterioration and can exhibit improper reinforcement detailing. In order to gain a better insight into the impact of local corrosion, anchorage cracking, limited amounts of provided shear reinforcement, and improper reinforcement detailing, a test program was designed. Full-scale tests on nine half-joint beams were performed.

The results of the study show that even though the impact of an individual shortcoming on the load carrying capacity of reinforced concrete half-joint beams might not be substantial, inspectors and assessors should pay attention to the possibility of combined effects. When multiple deterioration processes are noted and/or questions are raised with respect to the reinforcement detailing, the impact on the load carrying capacity of the beam might be larger than the linear combination of the individual effects.

© 2017 The Authors. Published by Elsevier Ltd. This is an open access article under the CC BY license (<http://creativecommons.org/licenses/by/4.0/>).

1. Introduction

The design of bridges incorporating half-joints (also known as dapped end beams) is characterised by local reductions in the overall depth of the beam at the supports as shown in Fig. 1. Half joints were particularly popular in the UK in the 1960s and 1970s, leading to over 400 concrete bridges with this type of joint being built on the existing UK Highways England network [1,2]. The main reason for their popularity was that the structural form was suitable for pre-cast bridge construction [3]. In addition, an overall reduced construction depth was achieved with a level running surface along the bridge deck and the support spans.

However, the design configuration of half-joints has certain disadvantages. One of the most commonly reported issues is linked to the water tightness of the joint itself [4,5]. In most bridges that are inspected, the water tightness is not fully achieved leading to seepage of chloride-rich water on to the nibs of the half-joint. Due to the half-joint layout, this water can stagnate on the lower nib of the joint creating a beneficial environment for corrosion.

Nicholas [6] reported the inspection details for two reinforced concrete half-joint bridges in Australia. In both bridges, severe signs of deterioration were noted. In the first bridge, a lack of water

tightness in the small movement joints (and hence seepage onto the steel bearings and spreader plates) led to severe corrosion of the bearings and surrounding concrete. In the second bridge, cracks were noted in the concrete on both the upper and lower half-joint nibs. These cracks were partly attributed to the improper placement of the bearings and partly to reinforcement corrosion. In both cases, extensive interventions were required to repair the bridges. Similar problems were reported by Santhanam [7] in a bridge inspected in New South Wales where all the half-joint beams located on the outside of the bridge showed visible signs of cracking and water ingress.

The corrosion of the nib reinforcement can sometimes be severe as shown by Smith [8]. During the refurbishment of the old Medway Bridge in the UK, inspections revealed reinforcement section losses of up to 50% for the front-face hanger reinforcement. In addition, some bars showed insufficient anchorage and poor reinforcement detailing. However, it should be emphasized that despite these shortcomings no visible signs of distress were noted by Smith [8].

One of the most well-known examples of a bridge designed with half-joints is de la Concorde Overpass in Quebec (Canada). In 2006, the overpass collapsed killing five people [9]. The investigation following the collapse revealed that the bridge had collapsed due to the simultaneous occurrence of a number of different aspects, where none of these on their own would have led to the collapse [10]. Some of the contributing factors were

* Corresponding author.

E-mail address: Pieter.Desnerck@eng.cam.ac.uk (P. Desnerck).

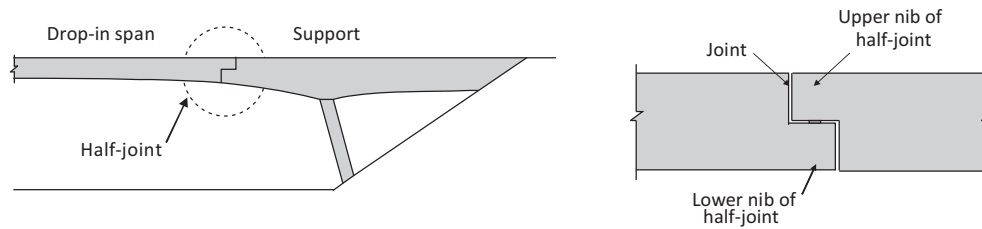


Fig. 1. Half-joint principle for reinforced concrete bridges.

the misalignment of certain reinforcing bars, improper repair methods and crack initiation due to deterioration along the top reinforcing bars.

Given the vulnerability of half-joints to deterioration, the development of maintenance strategies for half-joints is further hampered by the difficulty in inspecting half-joints due to limited access [7,11]. The only faces available for inspection are the outer vertical faces. The interior and transverse vertical faces can either be inaccessible or only conducive to limited access e.g. using snake eye cameras.

Limited guidance is available for the assessment of concrete half-joints [1,2,12]. These documents mainly relate to the effects of corrosion and crack widths. Fib bulletin 10 [13] identifies three different effects caused by corrosion: a reduction in the steel reinforcement bar diameter, the formation of a weak layer of corrosion products between the reinforcing bar and surrounding concrete, and cracking of the concrete surrounding the reinforcing bar. Both the weak layer at the concrete-steel interface and concrete cracking (due to the expansive nature of the corrosion products) result in a reduction in bond strength.

BA51 [14] provides guidance on the assessment of concrete structures affected by steel corrosion. A distinction is made between local and general corrosion. In the case of local corrosion, the steel section loss is identified as the main consequence. Assessors are advised to ignore locally corroded steel flexural and shear reinforcement which should be assumed to have no strength. Due to a reduction in ductility, these bars should also not be considered effective in plastic analyses. In addition, BA38 [15] points out that a reduction in fatigue life can be expected in reinforcing bars with deep pits caused by corrosion.

General corrosion often leads to only minor reductions in the bar cross-sectional area. In BA51 [14] it is advised, in cases where significant reductions are noticed, to account for general corrosion in a manner similar to local corrosion. However, the main effect of general corrosion tends to be the loss of bond strength due to the appearance of cracks along the bars. In this case, it is advised to reduce the bond strength of reinforcing bars associated with longitudinal cracks by 30%. In cases where spalling or delamination has occurred, the bond with the bars in the plane of delamination should be ignored. A reduction in fatigue life is less of a concern for general corrosion cases [15].

BA39 [16] specifically addresses the assessment of reinforced concrete half-joints. A distinction is made between serviceability checks (which are mainly based on crack width control) and ultimate limit state calculations which take into account actual reinforcement layouts. The guideline addresses deterioration effects by accounting for the loss of the cross-sectional area of reinforcing bars when evidence of corrosion is present. Specific reference is made to BD38 [15] when fatigue checks are required. However, a possible reduction in anchorage capacity due to corrosion is not explicitly addressed.

As design codes and standards are developed primarily for new construction, assessors of existing structures have to rely on the

documents such as those previously mentioned to obtain guidance about how to account for corroded reinforcing bars in existing reinforced concrete structures. Although extremely useful, these documents have been developed based on a limited amount of data. Furthermore, none of the guidelines directly address the potential synergistic effects that might occur when e.g. concrete deterioration, corroding reinforcing steel and/or improper detailing are simultaneously present in a structure.

Reinforcement layout and detailing deficiencies can exist in older half-joint structures, as shown in the past by inspections that revealed discrepancies between as-designed and as-built reinforcement layouts [7]. These inconsistencies may include missing reinforcing bars, relocated reinforcement and/or improper execution of reinforcement detailing (e.g. anchorages). Over the last decades, provisions with respect to detailing have changed significantly as well, resulting in structures which were considered properly detailed at the time of construction but are questionable based on the current knowledge and requirements [17]. The effect of the omission of specific rebars was the subject of a previous study by the authors [18], while anchorage defects are of particular interest in current work. In order to identify the impact that anchorage conditions can have on the behaviour of half-joint beams, bars where hooked ends are present or not, as well as prematurely curtailed longitudinal bars, were considered.

A further challenge with existing structures is that they have potentially been in service for decades and there is difficulty in recreating time-dependent deterioration processes. Corrosion, for example, causes in the first instance corrosion products to be formed leading to a reduction in the local reinforcement bar diameters. Over time the expansive nature of the corrosion process also leads to cracking and potentially spalling of the concrete [13]. Temperature loading on the other hand, especially in cases with frost-thaw cycles combined with the use of de-icing salts, may result in micro-cracking of the concrete and hence concrete strength reductions [19]. Rather than trying to recreate and accelerate the deterioration processes themselves, in the current work, the approach was to look at deterioration outcomes and hence to incorporate reinforcing bars with reduced sections or surrounded by cracked concrete.

After identifying the impact of these commonly found individual shortcomings, the next stage is then to look at the combination of deterioration and detailing deficiencies and start to provide the basis for guidance to assessors.

2. Experimental design

To provide data on the effect of deterioration mechanisms and to evaluate synergistic effects, an experimental program was designed. A total of nine full-scale reinforced concrete half-joint specimens were tested to failure to determine their load-carrying capacity and detailed behaviour. The results of the program are discussed in this paper.

2.1. Specimen geometry and reinforcement layout

In order to limit size effects, full-scale specimens were tested. The beams had a full height of 700 mm and width of 400 mm. At the nib, the height was reduced to 325 mm as can be seen in Fig. 2. The specimens were designed as beams with two different half-joint ends, resulting in two test scenarios for each beam.

2.1.1. Reference specimens

The reinforcement in the reference beam was designed according to the strut-and-tie approach, and consisted of U-shaped bars, shear stirrups, diagonal bars, longitudinal steel reinforcement and 3-legged vertical shear links in the full-depth section of the beam (B-region), as can be seen in Fig. 2.

Two specimens with a standard reinforcement layout were cast, one with a normal strength concrete (NS-REF) and one with a sub-standard low concrete compressive strength (LS-REF).

In addition to the properly detailed beams NS-REF and LS-REF, seven more specimens were tested which incorporated different deterioration defects and reinforcement detailing. Five specimens cast with normal strength concrete were designed to focus primarily on individual shortcomings, whereas an additional two beams made with lower strength concrete combined different defects to enable the synergistic effects to be investigated. An overview of the different test scenarios is given in Fig. 3.

2.1.2. Reinforcement layout and detailing

To evaluate the influence of the reinforcement detailing, a specimen with a reduced number of shear links (NS-RS) and a specimen where the diagonal bars were not properly anchored (NS-AD) were cast. In the NS-AD specimen, the diagonal bars were curtailed resulting in straight bars without bends. In the case of NS-RS, the second and fourth shear link away from the nib were removed (see Fig. 3).

2.1.3. Deterioration

As mentioned previously, the inner nib region of reinforced concrete half-joints is susceptible to the local corrosion of the reinforcing bars due to stagnating chloride-rich water seeping through the bridge joint. As none of the reinforcing bars in the inner nib region of the specimen under investigation are anchored in the inner nib zone itself (see Fig. 2), the biggest effect on the load bearing capacity is expected to be due to a reduction in the bar diameters. Hence, in specimen NS-LR, the reinforcing bars at the nib were locally

milled down to 50% of their original diameters (this is consistent with reductions noted in the UK during inspections, which can be as high as 30–50%).

A second, commonly detected, deterioration problem, is the corrosion of the bottom longitudinal tensile reinforcement along its length, primarily in the end zones of the beam. Over time, the corrosion process leads to concrete cracking that might manifest itself as spalling of the concrete cover layer over the full width of the beam, or more localised spalling at the corners resulting in anchorage problems.

Two different techniques were used to simulate these types of crack formation in the anchorage zone along the longitudinal steel.

The first approach was the introduction of a thin plastic sheet on top of the longitudinal reinforcing bars during casting to simulate a full-width crack (NS-PS&AL). The method of introducing plastic sheets to create weak planes has been successfully used by other researchers [20] (see Fig. 4). A carefully designed formwork system and casting sequence shown schematically in Fig. 4 allowed for the placement of a thin polyethylene sheet over the final 400 mm of the bars and the full width of the beam. In this way, an artificial crack was created in the anchorage zone.

In the second approach (NS-CC&AL), the aim was to generate a more localised crack pattern in the corners. Building on a technique developed by the authors for creating cracks along the reinforcing bars [21], concrete cylinders with a diameter of 62 mm were cast around the longitudinal reinforcing bars in the anchorage zone region prior to insertion in the beam formwork. The cylinders had a length of 110 mm with a 10 mm spacing in between to allow for the subsequent placement of the shear stirrups. Seven days after casting, the cylinders were subjected to two phases of split tensile tests to create cracks in the concrete along the reinforcing bar at 90-degree angles (see Fig. 5a & b). The force needed to create these cracks was a constant value of 17.5 kN.

After the pre-cracking phases, the bars were installed in the formwork before casting the full-scale beams (14 days after casting the cylinders). Previous research [21] had proven that a ring of intact concrete around a pre-cracked cylinder can provide significant confinement and reduce the impact of the cracking, hence in the full-scale experiments, a 1.5 mm thick metal sheet was introduced below the concrete cylinders (Fig. 5c) to mitigate the generation of hoop stresses.

The number of longitudinal bars in the anchorage zones varied in the different specimens as shown in Fig. 6. In specimens NS-REF, LS-REF, and the specimen with local bar reductions NS-LR, five longitu-

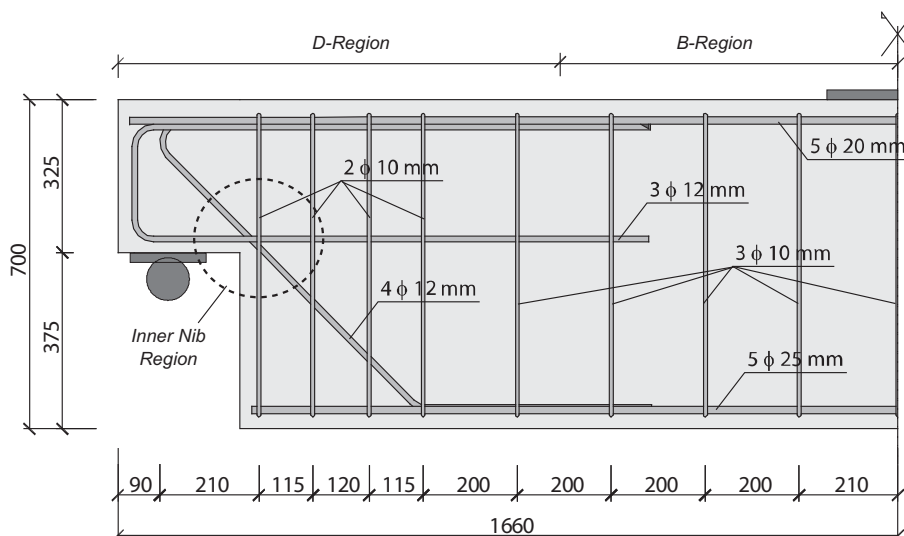


Fig. 2. Geometry and dimensions of experimental half-joint specimens NS-REF and LS-REF.

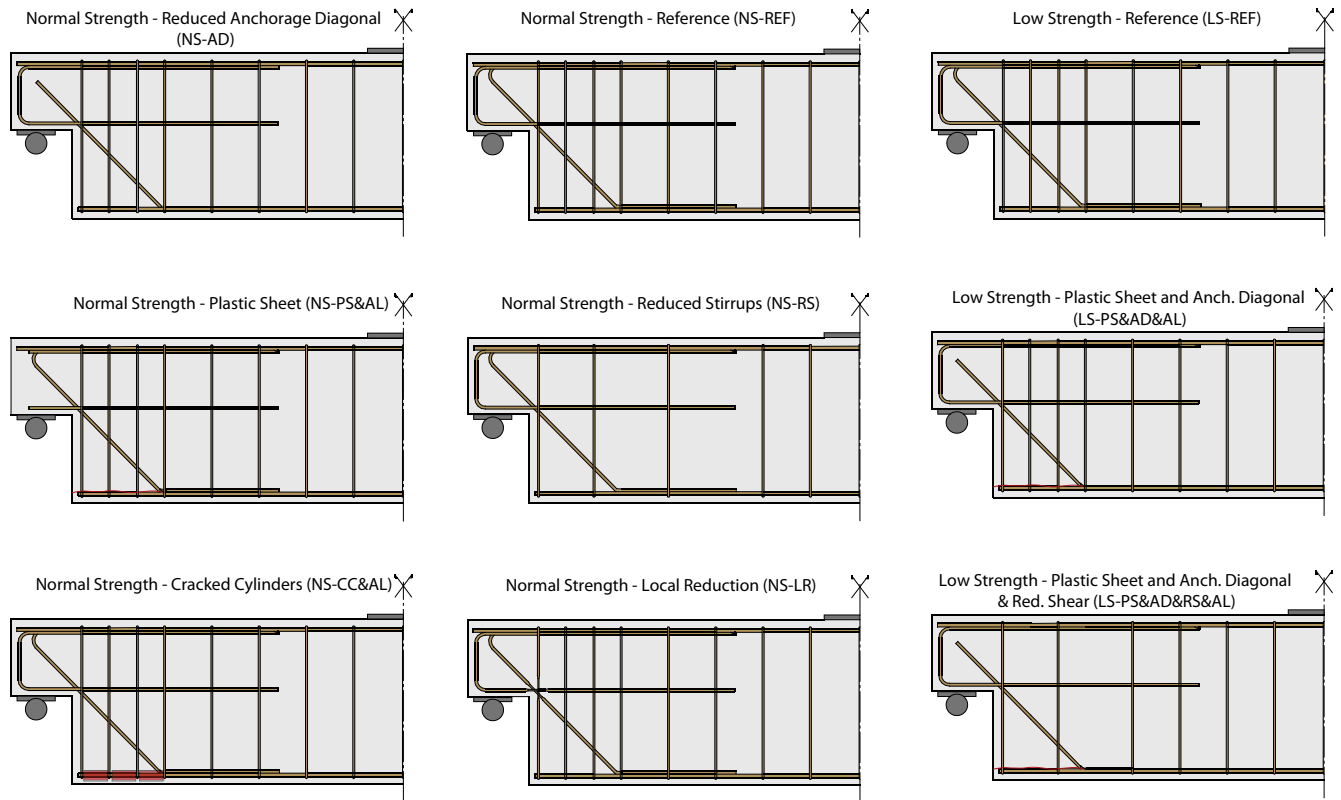


Fig. 3. Reinforcement layout for the different half-joint specimens.

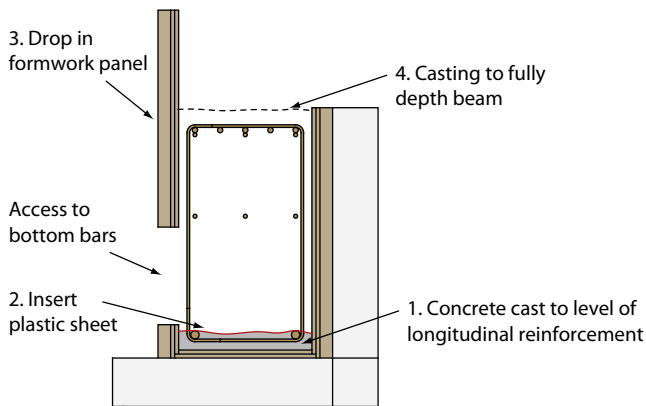


Fig. 4. Specimen NS-PS&AL: formwork design principle.

dinal reinforcing bars were provided along the full length of the beam. In the specimens designed to study the effect of cracking in the anchorage zone, only 2 bars were extended along the full length. The middle three bars were curtailed at the location at which the diagonal reinforcing bars intersected with the bottom longitudinal reinforcement. These specimens are designated with '&AL'.

2.1.4. Synergistic effects

In order to study the synergistic effects of a combination of detailing shortcomings and deterioration mechanisms, two additional specimens were cast. Specimen LS-PS&AD&AL combined a reduced anchorage length of the diagonal bar with the improper anchorage of the longitudinal reinforcement due to cracking (by means of a plastic sheet). In specimen LS-PS&AD&RS&AL, the specimen was further weakened by also reducing the amount of shear reinforcement.

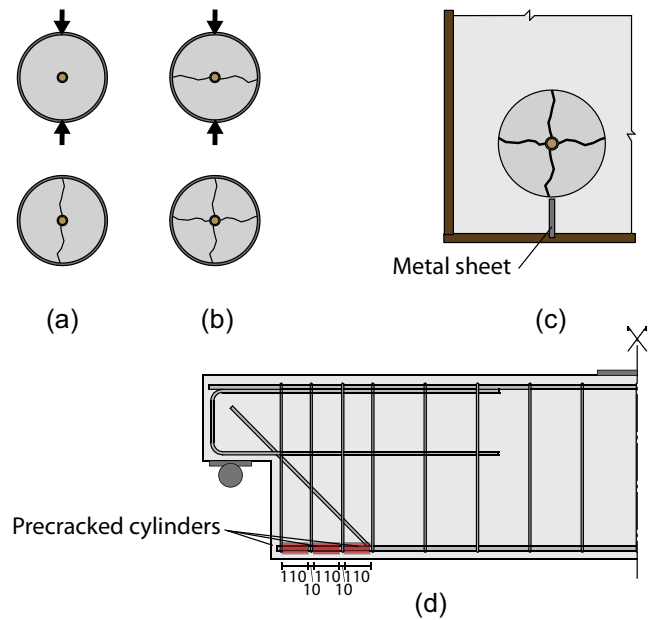


Fig. 5. Pre-cracking procedure for concrete in anchorage zone of half-joint NS-CC&AL: (a) pre-cracking phase I, (b) pre-cracking phase II, (c) casting cylinders within full-scale beams, and (d) side view of final anchorage zone.

2.2. Materials

Two types of concrete were used: a low strength (LS) C12/15 mix and a normal strength (NS) C30/37 according to European strength classes [22]. The concrete was mixed on site in a volumetric truck.

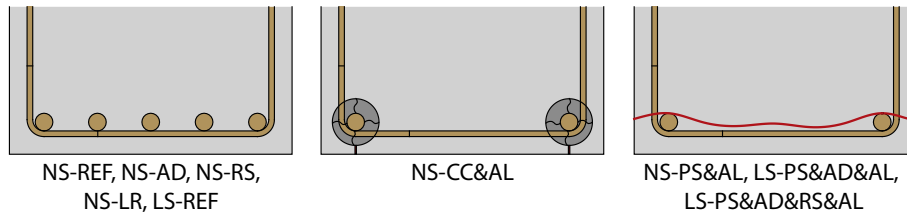


Fig. 6. Detail of anchorage zone concepts for different half-joint specimens.

The desired workability class for the normal strength concrete was achieved by adding a polycarboxylate ether (PCE) superplasticiser. The mix compositions can be found in Table 1.

All the beams were cured while hardening, demoulded after 72 h and stored in standard lab conditions at 21 ± 2 degrees Celsius and a relative humidity of $70 \pm 10\%$. Compressive strength tests were performed on control cubes with sides of 100 mm ($f_{c,cub}$). In addition to the compressive strength, the flexural ($f_{ct,fl}$) and split tensile strength ($f_{ct,sp}$), as well as the modulus of elasticity (E_c) were measured. The results can be found in Table 2.

Four types of ribbed reinforcing bars were used. The smaller reinforcing bars (10 mm or 12 mm) were cold deformed, while the larger bars were hot rolled.

The properties of the reinforcing bars, as measured in the laboratory in accordance with ISO 15630-1 [24], can be found in Table 3.

For specimen NS-LR, the diagonal bars, the U-bars, and the stirrup closest to the re-entrant corner were locally milled down to half of their cross-sectional area. The reduced zone was 100 mm long, extending 50 mm in both directions from the location where the U-bars, diagonal bars, and first stirrup cross. A tapered zone with a length of 10–15 mm was provided allowing for a smooth transition between the full bar cross section and the reduced section.

2.3. Test sequence and instrumentation

A 3-point bending test was performed on all the specimens, applying a load in the centre of the specimen (in contrast to [26]). As recommended by Clark and Thorogood [25] steel roller

Table 1
Concrete mix composition.

	Type	Amount [kg/m ³]	
		NS	LS
Cement	CEM I [23]	320	220
Coarse aggregate	4/10 mm uncrushed gravel	1058	1068
Fine aggregate	0/4 mm	829	864
Admixture	Superplasticiser	1.6	0.0
Water	–	170	198

Table 2
Mean and standard deviation (in brackets) of 28-day concrete properties for the different beams.

	NS-REFNS-LR	NS-RSNS-AD	NS-CC&ALNS-PS&AL	LS-REF	LS-PS&AD&ALLS-PS&AD&RS&AL
$f_{c,cub}$ [MPa]	50.8 (1.0)	35.8 (1.1)	41.0 (1.0)	15.4 (3.0)	18.3 (0.2)
$f_{ct,sp}$ [MPa]	3.83 (0.25)	3.45 (0.27)	3.49 (0.23)	2.23 (0.19)	2.28 (0.14)
$f_{ct,fl}$ [MPa]	4.84 (0.11)	4.63 (0.57)	5.08 (0.14)	2.61 (0.12)	3.54 (0.11)
E_c [GPa]	34300 (3850)	–	32500 (600)	28500 (3300)	24400 (1400)

Table 3
Mechanical and geometric characteristics of the reinforcing bars.

ϕ [mm]	f_y [MPa]	f_u [MPa]	h_r [mm]
10	539	596	0.75
12	529	559	0.99
25	578	674	1.59

bearings were used. They had a diameter of 90 mm and were supported in $450 \times 140 \times 30$ mm steel plates (Fig. 7).

All specimens were loaded in two phases (Fig. 8). In the first phase, the load on the specimens was increased stepwise until failure in one of the two nibs occurred. The applied load increments were 50 kN until first cracking after which the step size was decreased to 25 kN. As soon as one end of the specimen had reached its failure load, the specimen was unloaded. The support on the failed end was moved inwards supporting the full depth section of the beam. If necessary, additional strengthening of the failed end was provided. During the second testing phase, the load was once again applied stepwise in steps of 50 kN until the earlier applied load was reached after which the step size was decreased to 25 kN.

The applied load was measured by means of load cells located underneath both of the supports. The deflections were monitored using 7 transducers placed along the length of the beam. Strains at several locations along the reinforcing bars were continuously measured using strain gauges with a gauge length of 3 mm that had been pre-installed on the bars. For each location, one strain gauge was placed on the outermost reinforcing bar on one face and one on the outermost reinforcing bar on the other face (hence two measurements were available for each location). On average 30 strain gauges were installed per tested half-joint (Fig. 9). The strain gauges were designated SG followed by an indication of the bar on which they were installed (DIA for diagonal, UBAR for U-Bar, ST for stirrup, and BOT for bottom longitudinal bars) and a position indicator ranging from P0 to P7.

After each load increase, the concrete surface strains were manually recorded by means of DEMEC measurements (200 mm grid) on one side face of the beam. The crack pattern was also marked on the beam during testing.



Fig. 7. 3-Point bending test setup for half-joint beams.

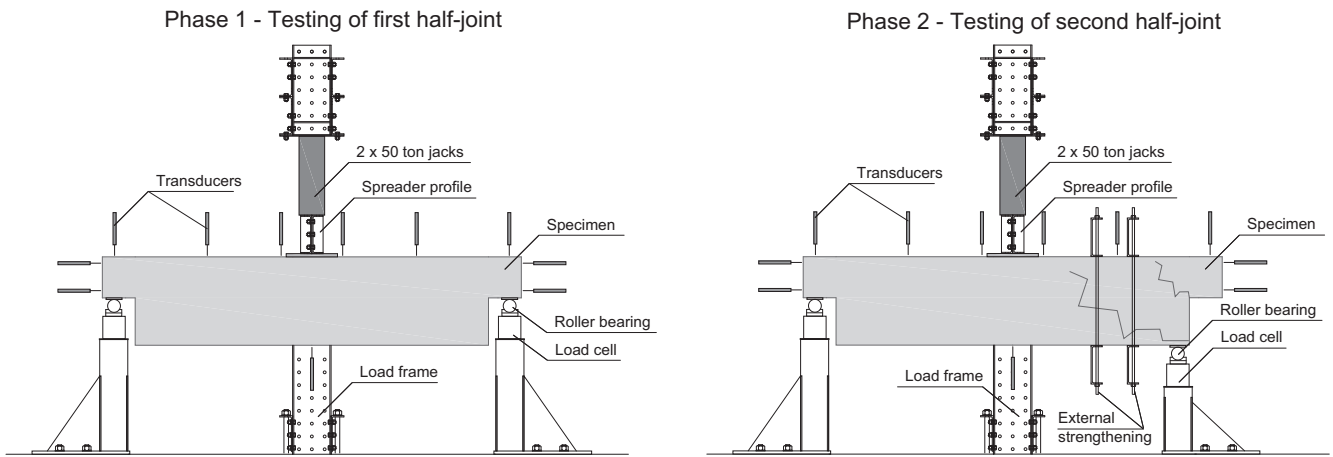


Fig. 8. Test set-up for 3-point bending experiments on reinforced concrete half-joint specimens.

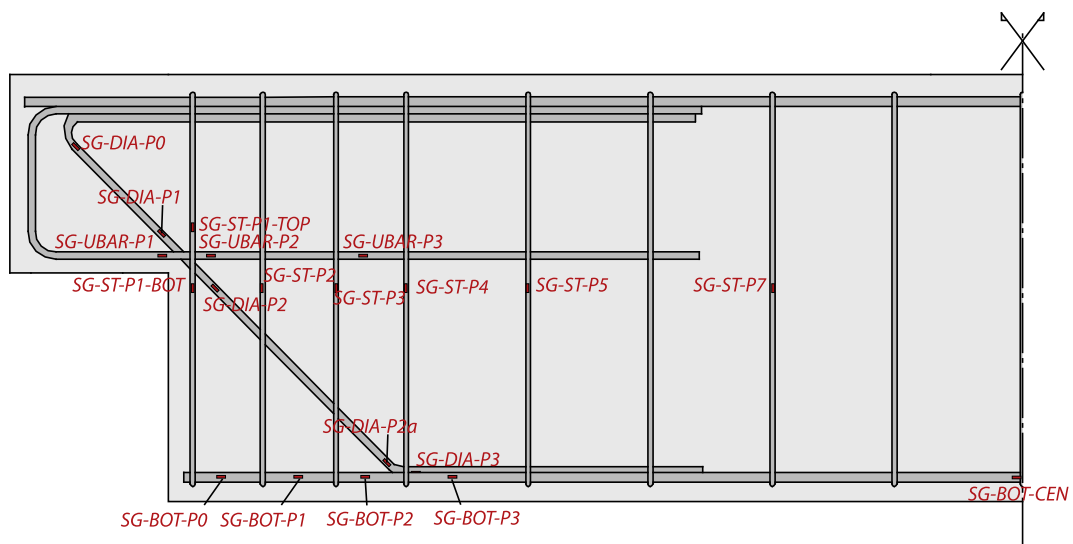


Fig. 9. Locations of the applied strain gauges.

3. Results

3.1. Overall behaviour

All the beams were tested until failure. The failure loads (defined as the maximum load applied on a half-joint) are shown in Fig. 10. The reference specimen NS-REF reached a failure load of 402.3 kN, whereas the reference specimen with a lower compressive strength reached a failure load of 400.0 kN. This indicates that for the studied geometry and reinforcement layout, a reduction of the concrete strength by ~15 MPa had little to no effect on the ultimate load carrying capacity. Both specimens failed due to the yielding of the reinforcing bars (diagonal bars, U-bars, and first stirrup) at the nib, leading to the rupture of these bars at failure.

Reducing the anchorage capacity of the diagonal bar turned out to have a negligible effect on the load carrying capacity for the studied geometry and reinforcement layout. With a failure load of 394.6 kN, the capacity of NS-AD can be considered similar to that of NS-REF and LS-REF. However, the failure mode of the half-joint changed from a nib failure to a full depth failure. The predominant crack appeared to be a shear crack that originated at the location where the diagonal bars and the longitudinal tensile reinforcement meet and then extended upwards at an angle of roughly 45 degrees.

The impact of reducing the shear reinforcement (from four two-legged stirrups to two two-legged stirrups in the zone closest to the nib) is more evident. The 358.7 kN failure load in NS-RS was more than 10% lower than that of NS-REF. As was the case for NS-AD, the dominant failure mode for NS-RS was a shear failure in the full depth section of the beam.

The effect of artificial cracks along the bottom longitudinal reinforcement led to strength losses between 4.5% and 9%, with the biggest reduction occurring when the cracked cylinder approach was used. Both the NS-CC&AL and NS-PS&AL half-joints failed due to an anchorage failure along the bottom longitudinal reinforcement and a clear crack formation in this anchorage zone was observed (discussed later).

The greatest reduction in load carrying capacity for the normal strength beams was found in NS-LR, the half-joint where the bar diameters had been locally reduced. The 50% reduction in the bar diameters of the U-bars, diagonal bars, and first shear stirrup led

to a failure load of 261.9 kN which was 65.1% of the capacity of the reference specimen NS-REF. As expected, this half-joint failed at the nib due to the yielding, and finally the rupture, of the reinforcing bars with the reduced cross-sectional areas.

When combining different defects, the impact on the load carrying capacity turns out to be more significant, indicating synergistic effects are present. Reducing the concrete strength in isolation had little to no effect on the strength (LS-REF) and the artificial crack introduced by means of a plastic sheet inserted in the anchorage zone led to a strength reduction of only 4.5% (NS-PS&AL). However, the combined effect of a low concrete strength and anchorage deficiencies (LS-PS&AD&AL) reduced the load carrying capacity to 234.9 kN, 60% of that of NS-REF. The dominant failure mode was the debonding of the longitudinal reinforcement.

If in addition, the amount of shear reinforcement provided was reduced (LS-PS&AD&RS&AL), the load carrying capacity dropped further to only 42.5% of the capacity of the reference specimen. This additional drop of ~20% is bigger than the drop of 10% noted between NS-REF and NS-RS (when only the shear reinforcement was reduced), which indicates that the reduction in shear reinforcement also reduces the confinement provided along the bottom reinforcement hence leading to a significant decrease in anchorage capacity.

Fig. 11 shows the load-deflection curves for all the specimens. The beams cast with normal strength concrete are shown in Fig. 11(a) while those with low strength concrete are shown in Fig. 11(b). The plotted deflection is the total deflection measured between the support and the end of the disturbed region (700 mm into the full-depth section). In this way, the effect of relocated supports for those half-joints that failed in the second loading phase is minimised.

For all specimens, an almost linear relationship is measured until the point of first cracking. At a load between 100 kN and 125 kN cracks started to develop at mid-span and at the inner corner of the nib leading to a deviation from the initial linear load-deflection behaviour. No significant difference was found between the loads at first cracking for the normal strength and low strength specimens.

With increasing load, the deflection of the specimens increased gradually. For most of the specimens, the failure occurred in a semi-brittle way. The largest deflections were measured in the reference specimens which also showed some ductile behaviour due

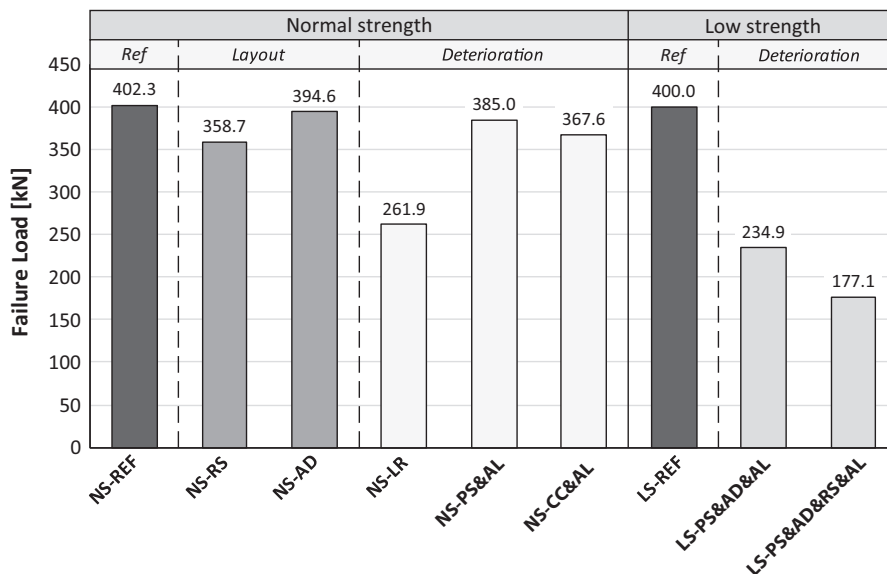


Fig. 10. Failure load of the different half-joint specimens.

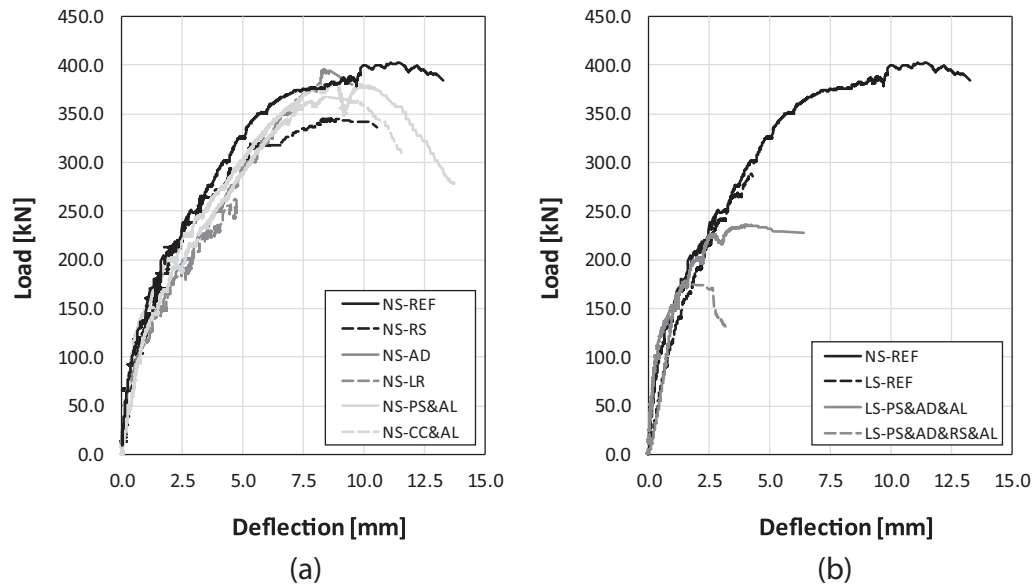


Fig. 11. Load-Deflection curves for specimens (a) with normal strength concrete and (b) with low strength concrete.

to the yielding of the reinforcing bars. However, even for the reference specimens, the final deflections were still relatively small (<15 mm).

3.2. Crack formation

As mentioned previously, with the exception of specimens NS-REF, NS-LR, and LS-REF which failed in the nib, the specimens failed due to an anchorage failure along the bottom reinforcement bars. Fig. 12 shows the crack patterns where the dominant cracks at the moment of failure are indicated in bold. Hatched areas are locations where the concrete cover spalled off either during testing or at the moment of failure.

The dominant crack initiated at the inner nib for specimens NS-REF, NS-LR, and LS-REF and occurred at an angle of ~ 45 degrees with the beam axis. Specimen NS-RS failed in shear, with the dominant shear crack running from the lower outer corner of the full-depth section and crossing the remaining shear links at an angle of ~ 45 degrees.

For specimens NS-CC&AL and NS-PS&AL, a clear crack was visible along the bottom longitudinal reinforcement prior to failure. For specimen NS-PS&AL this crack, which extended over the full width of the specimen, was most visible on the front face of the beam reflecting the plastic sheet that was inserted at the level of the reinforcement. For half-joint NS-CC&AL, the crack was visible along the full anchorage length as well but remained within the concrete cover at the corner rather than extending the full width of the beam. Just prior to failure, the corner concrete cover of NS-CC&AL spalled off leading to a significant reduction in anchorage capacity and hence the failure of the beam. A detailed view of the crack patterns at the end face is shown in Fig. 13 for half-joints NS-PS&AL and NS-CC&AL.

3.3. Stress distribution

Based on the strain gauge measurements and the measured Young's moduli, the steel stresses at each load step can be calculated. In the reference beams, all the reinforcing bars at the inner nib are yielding before the failure of the beam. The stresses in all the bars increased simultaneously and the bars yielded shortly before rupture indicating that none of the reinforcing bars reached their capacity prematurely.

For specimen NS-LR with bars with a locally reduced cross-sectional section, the steel stresses at a given load are significantly higher than the stresses at the same location and same load level for the reference beams, which was to be expected. The total force taken by the individual bars is comparable hence leading to higher steel stresses and the bars in NS-LR reaching yield at a lower load level.

Fig. 14 shows the evolution of the steel stresses in the longitudinal bottom reinforcement for NS-REF at several locations along the length of the bar (see Fig. 9 for an indication of the locations). The plotted stresses are based on the averaged strains for each location (two strain gauges are present at each location). The highest steel stresses in the longitudinal steel bars were measured at the centre of the beam. As soon as the first cracks appeared (roughly at mid-span) a clear increase in the longitudinal mid-span stress was noted after which the stress increased almost linearly with the applied force. As the force increased, higher stresses were also recorded in the anchorage zone. The stress started to significantly increase at location P3 (adjacent to the location where the diagonal bars and longitudinal steel meet) at a load of around 175 kN. At a load of ~ 200 kN, a steep increase in the stress at location P2 was noted and, at a load of ~ 250 kN, also at location P1. After the steep increase in stress (which is related to the development of cracks in the zone of the strain gauge) the stresses increased in an almost linear way. The increase was, however, higher at location P2 than at location P3 due to the overlap of the diagonal bars and longitudinal bars at location P3, which play a significant role in carrying the load at that given location.

For the beam with the cracked cylinders (NS-CC&AL), a similar behaviour was noted for the strain gauge at mid-span. The load at which the stresses along the anchorage zone of the longitudinal reinforcement started to increase significantly was higher than for the reference specimen. However, the sudden increase in the stresses in the anchorage zone is significantly larger as well.

A similar observation can be made for the case where a thin plastic sheet is used as artificial crack (specimen NS-PS&AL). The sudden increase in steel stresses at location P2 and P3 occurs simultaneously and at a load level of ~ 200 kN. Even at location P1, the stress increases significantly at this load, indicating that almost the entire anchorage zone is instantly activated. Close to failure, the stresses at location P3 exceed the stresses at mid-span, while a small relaxation is noted nearer to the end of the bars

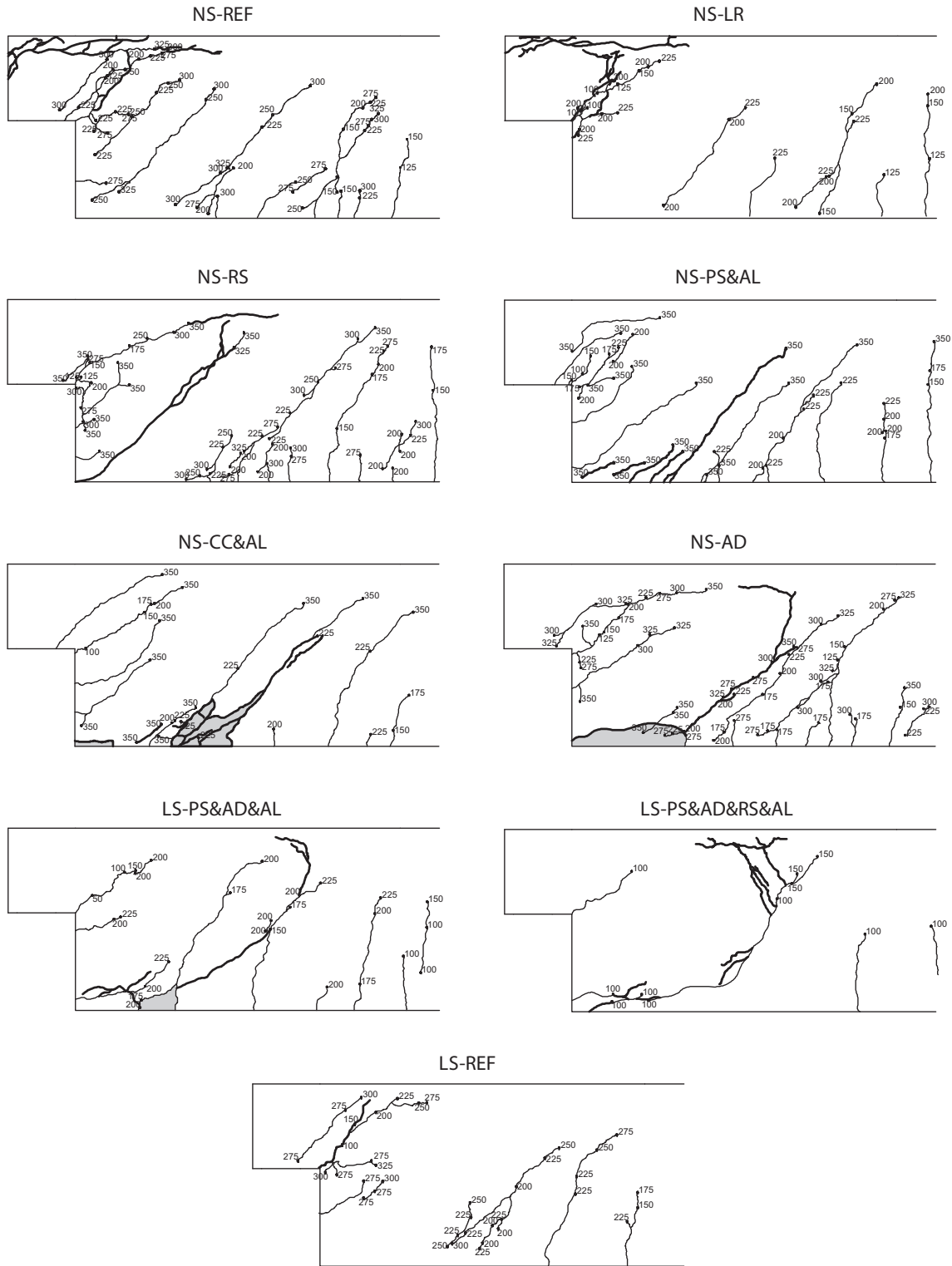


Fig. 12. Observed crack patterns for all specimen (bold lines are dominant cracks at failure).

(location P1 and P2). The stresses reached in the reinforcing bar, along the entire anchorage zone, are higher than those recorded for the reference specimen NS-REF.

It should be emphasised, however, that for specimens NS-CC&AL and NS-PS&AL only two bars extended into the anchorage zone whereas for beam NS-REF all 5 bars ran along the full length of the beam. This means that, despite the higher reinforcing steel

stresses in specimens NS-CC&AL and NS-PS&AL, the total bar force taken by the longitudinal bottom reinforcement is highest in specimen NS-REF, as can be seen in Fig. 15. Whereas the bar forces are gradually increasing in the reference specimen, a much more sudden increase is noted for the specimens with artificial cracks. When a thin plastic sheet is used, the increase turns out to be slightly smaller, but occurs at a lower load, than when pre-cracked con-

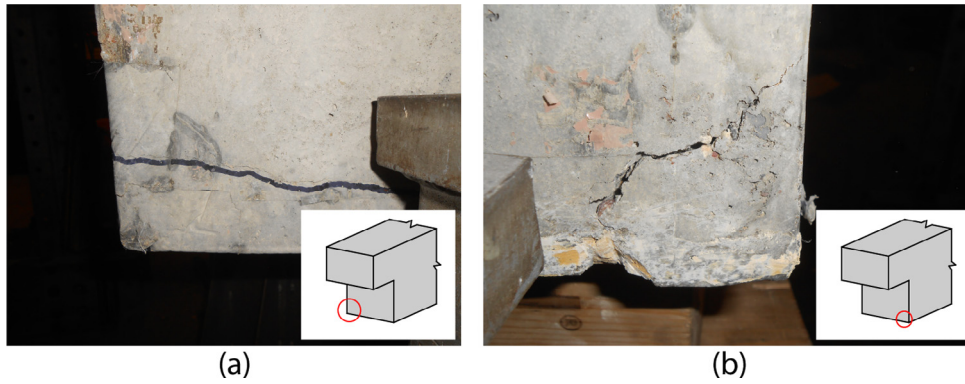


Fig. 13. Detail of the crack pattern developed on the end face of the beam at the anchorage zone for half-joint (a) NS-PS&AL and (b) NS-CC&AL.

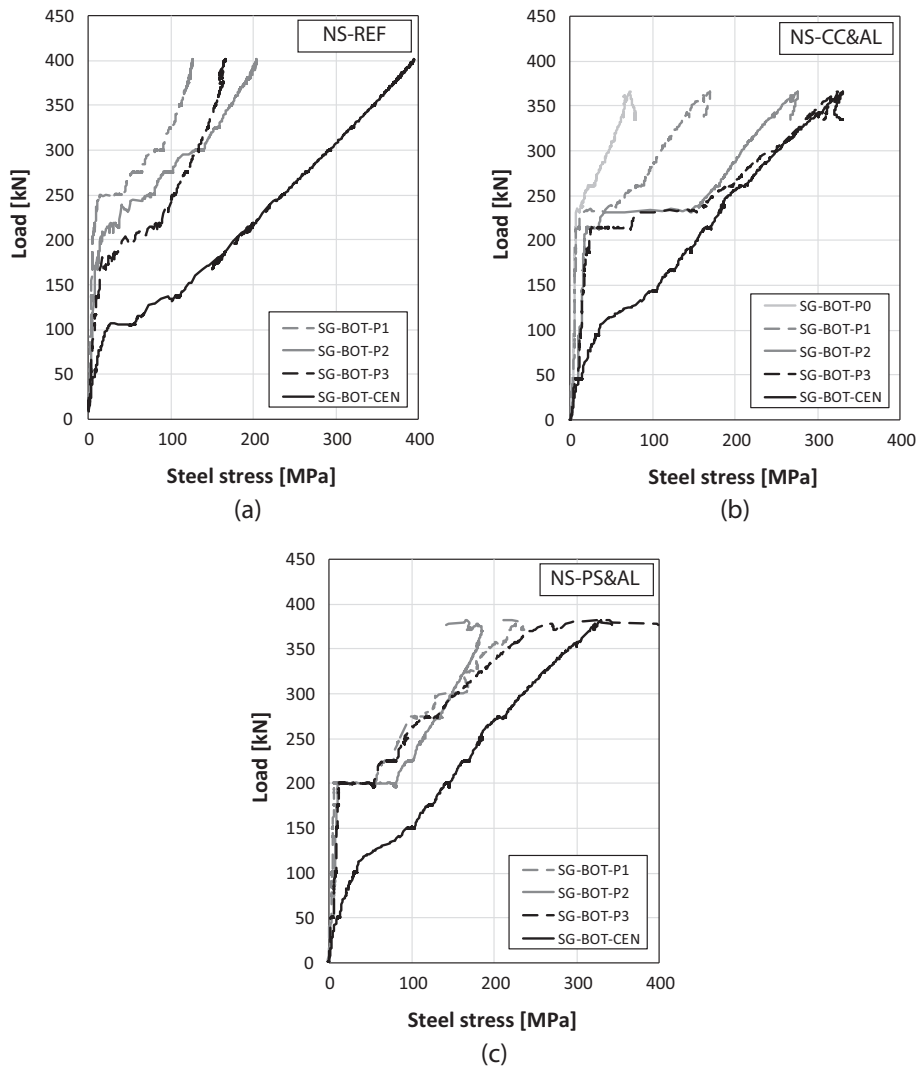


Fig. 14. Evolution of steel stresses along the bottom reinforcing bar for: (a) NS-REF, (b) NS-CC&AL, and (c) NS-PS&AL.

crete cylinders are used. The total bar forces at failure for the specimens with defects are more than 50% lower than in the reference configuration.

3.4. Synergistic effects

For the studied half-joint geometry, in a number of cases, the impact of individual shortcomings such as improper detailing and

deterioration turned out to be relatively small. Reducing the concrete strength did not result in a significant load carrying capacity drop, and the improper anchorage of the diagonal bars or insertion of cracks along the bottom bars resulted in a maximum strength reduction of 10%. Reducing the amount of shear reinforcement close to the nib reduced the capacity from 402.3 kN (NS-REF) to 358.3 kN (NS-RS). However, when several defects are combined, more significant reductions are noted indicating

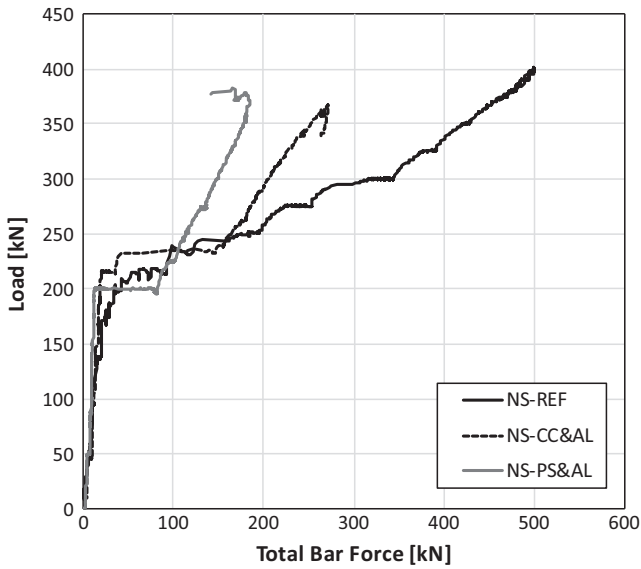


Fig. 15. Evolution of total bar force at location SG-BOT-P2 for specimen NS-REF, NS-CC&AL, and NS-PS&AL.

that the effect of defects is larger than their cumulative individual contributions.

In the current beams, for a given defect, the forces in the specimens are carried through alternative load paths resulting in only a relatively minor impact on the overall capacity. As mentioned previously, the total bar forces in the longitudinal bottom reinforcement, for example, are smaller when cracks are present in the anchorage zone (specimens NS-CC&AL and NS-PS&AL). This reduction in capacity is overcome by an increase in the diagonal bar forces, indicating a larger component of the force is diverted into the diagonal bars, resulting in a smaller demand on the anchorage.

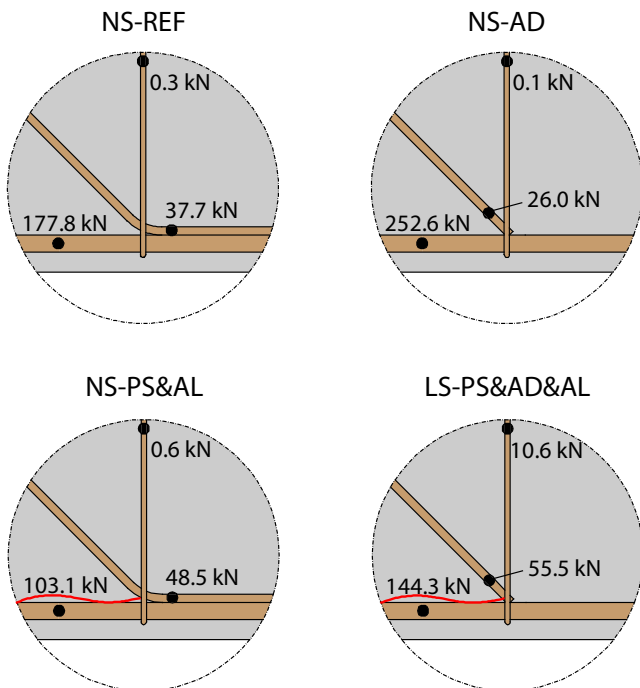


Fig. 16. Bar forces at the intersection of the longitudinal bottom reinforcement, diagonal reinforcement and fourth stirrup at a load level of 230 kN for specimens NS-REF, NS-AD, NS-PS&AL, and LS-PS&AD&AL.

Fig. 16 compares the bar forces at the intersection point of the diagonal reinforcement, longitudinal bottom reinforcement, and fourth stirrup. A load level of 230 kN was selected as, for all specimens shown, the failure load hadn't been reached but anchorage zone cracking was present leading to increased steel stress at the locations P2 and P3 along the longitudinal bottom reinforcement. None of the bars reached yielding at this stage (yield force for the 10 mm, 12 mm and 25 mm reinforcing bars were 42.3 kN, 59.8 kN, and 283.7 kN respectively).

The recorded total bar forces indicate that due to the reduced anchorage of the diagonal bars (NS-AD), the total force in the diagonal bars is slightly reduced from 37.7 kN to 26.0 kN when compared with the adequately anchored bars (NS-REF) at a load level of 230 kN. Consequently, the total force in the longitudinal bottom reinforcement increased. The impact on the total force in the stirrups was minimal.

When the anchorage capacity of the longitudinal bottom reinforcement was reduced by means of a thin plastic sheet (NS-PS&AL), an inverse trend was noted. In this case, the total force in the bottom bars dropped from 177.8 kN to 103.1 kN compared to the reference beam (NS-REF), while the total diagonal bar force increased from 37.7 kN to 48.5 kN.

When improper anchorage of the diagonal bar is combined with crack formation in the anchorage zone, both actions were noted. On one hand, the total bar force in the longitudinal bars reduced (however to a smaller extent than seen for NS-PS&AL) and on the other hand, the force in the diagonal bar increased. The total force in the diagonal bar reached a value of 55.5 kN at a location 15 mm from the end of the bar, leading to high bond stresses approaching the maximum anchorage capacity (the specimen failed at a load of 234.9 kN). A significant increase in the total force in the fourth stirrup occurred as well. This increase occurred in a rather sudden way as shown in Fig. 17.

If, in addition, the amount of shear reinforcement is reduced as well (as is the case in specimen LS-PS&AD&RS&AL), the sudden increase in bar forces in the anchorage zone occurring at a load of ~ 175 kN led to the failure of the specimen. The absence of the fourth stirrup did not allow alternative load paths to develop, leading to a failure load of 177.1 kN.

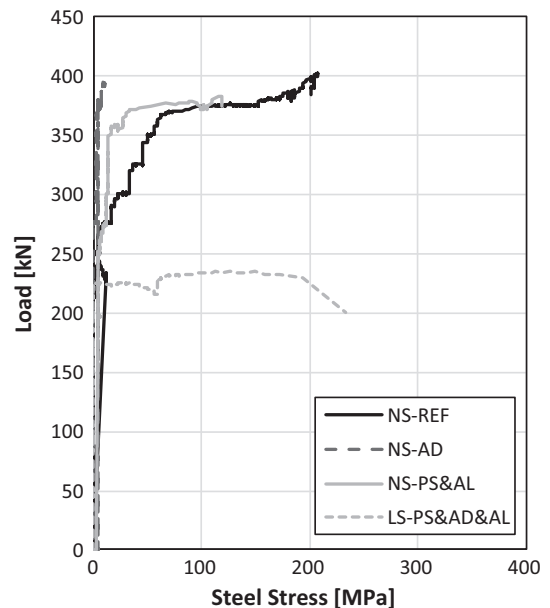


Fig. 17. Evolution of steel stresses in the fourth stirrup for specimens NS-REF, NS-AD, NS-PS&AL and LS-PS&AD&AL.

3.5. Implications for the assessment of half-joint structures

The assessment of existing reinforced concrete structures, and half-joints in particular, is a challenge. One visible outcome that can be observed during inspections is cracking that has extended to accessible external surfaces. The results of the current work suggest that, during inspections, special attention should be paid to the concrete condition and the existence and location of cracks in the nib area (inner nib), shear cracks close to the nib in the full-depth section and/or longitudinal cracks along the bottom reinforcement in the full-depth section. These cracks can be indicators of potential issues such as inadequate reinforcement and/or detailing, an overloaded structure, deterioration e.g. freeze-thaw damage, reinforcement corrosion, or can be signs of the existence of additional mechanical actions (support settlements, impact loads).

In some cases, one defect in an experimental beam led to a relatively minor reduction in the failure load. However, this outcome relied on having adequate concrete capacity and a significant number of effective reinforcing bars in the nib and full-depth section, such that alternative load paths could develop over time. When more than one defect was present in an experimental beam, in some cases, the reduction in the load carrying capacity was found to be greater than the summation of the individual defect reductions in isolation. This was a consequence of an absence of alternative load paths leading to a significant capacity reduction. Assessors and practising engineers are therefore advised to reflect on possible load paths. If there is an absence of alternative load paths, even a single defect could be much more critical than it was for the given reinforcement layout, concrete properties, beam geometry and deterioration outcomes investigated in the experimental beams presented here. In addition, if visual inspections and field tests indicate that improper detailing and deterioration exist simultaneously in a structure, consideration must be given to the potential for adverse synergistic effects.

Common methods for the design and assessment of reinforced concrete half-joints are based on strut-and-tie models (STM) [27] where the reinforcing bars are modelled as tensile ties and the concrete is modelled as compressive struts. Nodal checks (at locations where struts and ties meet) evaluate whether the concrete capacity is exceeded and/or proper anchorage of the reinforcing ties is provided. Details of STM modelling, potential ways of accounting for defects including limiting the tie capacity to reflect deterioration in the anchorage zone, and the correspondence of STM models with the experiments discussed above, will be published later. However, more work needs to be done to develop modelling tools to reflect deterioration outcomes and detailing layouts that are representative of structures in practice.

4. Conclusions

Most studies performed on half-joint beams have focussed on the design optimisation of new reinforced concrete beams and bridge decks. However, existing half-joint structures are vulnerable to deterioration processes and can exhibit improper reinforcement detailing. In order to gain a better insight into the impact of local corrosion at the inner nib, different degrees of cracking around the longitudinal tensile reinforcement, limited shear reinforcement, and improper reinforcement detailing, a test program studying these aspects was designed. Full-scale tests on 700 mm height, 400 mm wide half-joint beams led to the following observations:

- For the specimen geometry and reinforcement layout studied in the current work, the impact of the concrete strength on the load carrying capacity was negligible.

- A local reduction of 50% of the cross-sectional area of the diagonal, U and vertical reinforcing bars at the inner nib of the half-joint resulted in a 35% reduction in failure load compared to the reference specimen.
- Two methods for mimicking corrosion cracking of concrete around the longitudinal steel were implemented. Both methods; insertion of a plastic sheet at the level of the reinforcing bars and the inclusion of pre-cracked concrete cylinders, resulted in the failure of the full-scale half-joint specimens due to the debonding of the longitudinal reinforcement.
- The individual impacts of improper anchorage of the diagonal bar, a reduction in the provided shear reinforcement and cracks around the bottom longitudinal reinforcement each resulted in strength losses of approximately 10%.
- Whereas in isolation certain individual deficiencies had little or no effect, when combined, synergistic effects were noted. For example, the simultaneous occurrence of cracks along the longitudinal reinforcement and improper anchorage of the diagonal reinforcement led to a reduction in the overall capacity of the beam of 40%. For a beam where there was improper anchorage of the diagonal bars, cracking along the longitudinal steel, and only a limited amount of shear reinforcement, an additional decrease of 20% in the failure load was measured, resulting in a total capacity reduction of 60%.

The results of the study show that even though the impact of an individual shortcoming on the load carrying capacity of reinforced concrete half-joint beams might not be substantial, inspectors and assessors should pay particular attention to load paths and the possibility of combined effects. When multiple deterioration processes are noted and/or questions are raised with respect to the reinforcement detailing, the impact on the load carrying capacity of the beam might be larger than the linear combination of individual effects.

Acknowledgements

The authors would like to acknowledge the financial support of EPSRC – the Engineering and Physical Sciences Research Council (UK) – through the EPSRC Project ‘Reinforced concrete half-joint structures: Structural integrity implications of reinforcement detailing and deterioration’ [Grant no. EP/K016148/1].

Additional data related to this publication is available at the University of Cambridge’s institutional data repository: <https://doi.org/10.17863/CAM.13336>.

References

- [1] Transport Scotland. TS Interim Amendment No. 20 – Concrete half-joint deck structures; 2006. p. 23.
- [2] Loudon N. IAN 53/04 – Concrete half-joint deck structures; 2004. p. 18.
- [3] Mattock A, Chan T. Design and behavior of dapped-end beams. *PCI J* 1979;28–45.
- [4] Sarveswaran V, Roberts M, Anstice O. Reliability assessment of deteriorating RC bridge half joints. In: Proc 25th conf our world concr struct, Singapore, Singapore: CI-Premier PTE Ltd; 2000. p. 555–62.
- [5] NSW Government. Rehabilitation of Tarban Creek Bridge. Transport Roads & Marine Services; 2012.
- [6] Nicholson T. Design and construction of A34 Wolvercote highway viaduct replacement, UK. *Bridg Eng* 2014;167:122–30.
- [7] Santhanam B, Shah P. Concrete half joint bridges in New South Wales: challenges in risk management. In: Austroads Bridg Conf, Sydney; 2011. p. 497–511.
- [8] Smith D. Refurbishment of the old Medway bridge. *UK Proc ICE-Bridg Eng* 2005;158:129–39.
- [9] Mitchell D, Cook W. Rapport sur les causes techniques de l’effondrement du viaduc de la Concorde – Annexe A7 – Analyse de la conception des viaducs de la Concorde et de Blois; 2007.
- [10] Mitchell D, Marchand J, Croteau P, Cook W. Concorde overpass collapse: structural aspects. *J Perform Constr Facil* 2011;25:545–53.

- [11] Watson J. Acoustic emission monitoring of concrete structures. In: Elsener B, editor. Proc first work COST 534 NDT assess new syst prestress concr struct, Zurich, Switzerland; 2004. p. 31–44.
- [12] Clark L. IAN53 Half-Joint Assessment Advice – ULS Assessment of half-joints. Highways Agency; 2010.
- [13] Task Group Bond Models. fib Bulletin 10 - Bond of reinforcement in concrete. Lausanne; 2000.
- [14] The Highways Agency. BA 51/95 – The assessment of concrete structures affected by steel corrosion; 1995.
- [15] Department of Transportation. BA38/98 – assessment of the fatigue life of corroded or damaged reinforcing bars, vol. 16; 1993.
- [16] Department of Transportation. BA39/93 Assessment of Reinforced Concrete Half-joints; 1993, vol. 22.
- [17] Mitchell D, Cook W, Peng T. Importance of reinforcement detailing. *ACI Spec Publ* 2010;273:1–16.
- [18] Desnerck P, Lees J, Morley C. Impact of the reinforcement layout on the load capacity of reinforced concrete half-joints. *Eng Struct* 2016;127:227–39.
- [19] fib Bulletin 65 - Model Code 2010 – Final Draft – vol. 1; n.d.
- [20] Reilly J, Cook W, Bastien J, Mitchell D. Effects of delamination on the performance of two-way reinforced concrete slabs. *J Perform Constr Facil* 2014;28:8.
- [21] Desnerck P, Lees J, Morley C. Bond behaviour of reinforcing bars in cracked concrete. *Constr Build Mater* 2015;94:126–36.
- [22] European Committee for Standardization. EN 1992-1-2 Eurocode 2: Design of concrete structures – Part 1–2: General rules - Structural fire design. European Committee for Standardization; 2008.
- [23] European Committee for Standardization. EN 197-1:2011 – Cement – Part 1: Composition, specifications and conformity criteria for common cements, Brussels, Belgium; 2011.
- [24] ISO – International Organization for Standardization. EN ISO 15630-1, Steel for the reinforcement and prestressing of concrete—test methods—Part 1: Reinforcing bars, wire rod and wire; 2002.
- [25] Clark L, Thorogood P. Serviceability behaviour of reinforced concrete half joints. *Struct Eng* 1988;66:295–302.
- [26] Lu W, Yu H, Lin I. Behaviour of reinforced concrete dapped-end beams. *Mag Concr Res* 2012;64:793–805.
- [27] fib Task Group 4.4. fib Bulletin 45 - Practitioners' guide to finite element modelling of reinforced concrete structures. Lausanne, Switzerland: International Federation for Structural Concrete (fib); 2008.